International Journal of Physics, 2016, Vol. 4, No. 4, 106-112
Available online at http://pubs.sciepub.com/ijp/4/4/4

DOI:10.12691/ijp-4-4-4

Scattering Events and Heat Conductivity of Layered $La_{2-x}Sr_xCuO_4$ Superconductors

Rakhi Sharma[1], B. D. Indu[2,*], Pawan Kumar[1]

[1]Department of Physics, Gurukula Kangari Vishwavidyalaya, Haridwar-249401, India
[2]Department of Physics, Indian Institute of Technology Roorkee, Roorkee-247667, India
*Corresponding author: drbdindu@gmail.com

Abstract The problem of heat conduction in layered $La_{2-x}Sr_xCuO_4$ superconductor has been investigated in a new frame work of in-plane and cross-plane concepts with the help of modified Callaway model of thermal conductivity based on relaxation time approximation. Using the many body quantum dynamical theory of the expressions for thermal conductivity in context of in-plane and cross plane have been obtained and results are found in excellent agreement with experimental observations for layered $La_{2-x}Sr_xCuO_4$ cuprate superconductors. The theory explores the possibility of device fabrication cold in one direction and hot in the other.

Keywords: *relaxation times, in-plane and Cross- plane thermal conductivity, scattering process*

Cite This Article: Rakhi Sharma, B. D. Indu, and Pawan Kumar, "Scattering Events and Heat Conductivity of Layered $La_{2-x}Sr_xCuO_4$ Superconductors." *International Journal of Physics*, vol. 4, no. 4 (2016): 106-112. doi: 10.12691/ijp-4-4-4.

1. Introduction

A detailed understanding of thermal transport and management in layered systems is increasingly emerging as thrust area in the modern efficient energy technology and theorists are interestingly involved to explain this phenomenon. The study of heat transport in conventional and high temperature superconductors (HTS) emerged as an important tool to understand the scenario of phonon and electron energy spectrum along with various collision events. The thermal conductivity κ was understood in such systems contributed both by electrons and phonons in the form of electronic thermal conductivity κ_e [1] and phonon conductivity κ_{ph} [2] related by $\kappa = \kappa_e + \kappa_{ph}$. At fairly low temperatures the Widemann-Franz law often breaks down severely and the metallic behavior of solids which become superconducting suggests that the electronic thermal conductivity starts to disappear and one can take $\kappa_e \to 0$ negligibly small with $\kappa \simeq \kappa_{ph}$ instead of the concept of isolated channels [3,4,5]. The layered high temperature superconductor structures are highly anisotropic in character and thus the in-plane and cross-plane thermal transport becomes more and more important. Some investigations reveal [6,7] that scattering of electrons from phonons, impurities and interfacial roughness can be used to determine in-plane electron transport and resonant tunneling effects and the in plane scattering can be used to determine cross-plane transport [8,9,10] and this is further supported by the different phonon velocities in different directions [9]. Lattice vibrations can couple to each other and strongly couple with any structural defect, surface boundaries, dislocations or point defects [2,4,11,12,13,14,15].

The thermal conductivity of layered structures based on Boltzmann transport equation approach has studied by many theorists [16,17,18] using the method of relaxation time approximation (RTA). The validity of RTA, however, suffers from many adequacies because of its derivation for low frequency phonons at low temperatures, additivity of lifetimes of individual scattering events and its incompatibility to explain inelastic phonon scattering processes [18-24]. Adopting the quantum mechanical approach these inadequacies have been successfully removed from the phenomenological theories of thermal conductivity [18,20,21]. The discrepancies involved due to the phonon dispersion relation and violation of Matthiessen's rule of additivity of inverse relaxation time have been removed by introducing the equivalence between relaxation times and line widths [20,21]. The electron-phonon and the resonance scattering events are found to be highly sensitive in microstructures also, which successfully explain the abnormal behavior (dip and rise) of thermal conductivity curve at and above the critical temperature T_c. In this region an utmost care has to be taken as the thermal transport takes place in the presence of pairons in HTS which do not contribute to thermal conductivity.

In the present work we have investigated the role of various scattering processes based on many body quantum dynamics and the thermal conductivity is resolved into in-plane and cross-plane contributions which addresses the possibility of restricting the heat flow in a particular direction and allowing it in the another which can be exploited to the development of exotic technological HTS crystals for industrial use. In the present case in-plane

thermal conductivity is observed greater than cross-plane thermal conductivity.

2. Formulation of the Problem

The anisotropic considerations suggest that the thermal conductivity of a layered crystal can be resolved as a contribution of in-plane thermal conductivity $\kappa_{\parallel}$ and cross -plane thermal conductivity $\kappa_{\perp}$ as

$$\kappa = \kappa_{\parallel} + \kappa_{\perp} \tag{1}$$

where $\kappa_{\parallel}$ and $\kappa_{\perp}$ can be obtained from Callaway expression [2] using relaxation time approximation in the following form

$$\kappa_{\parallel} = \left(\frac{k_B}{2\pi^2 v}\right)\left(\beta^2\hbar^2\right)\int_0^{\omega_D} \tau_{k\parallel} \frac{\omega_{\parallel}^4 e^{\beta\hbar\omega_{\parallel}}}{\left(e^{\beta\hbar\omega_{\parallel}} - 1\right)^2} d\omega_{\parallel} \quad (1a)$$

$$\kappa_{\perp} = \left(\frac{k_B}{2\pi^2 v}\right)\left(\beta^2\hbar^2\right)\int_0^{\omega_D} \tau_{k\perp} \frac{\omega_{\perp}^4 e^{\beta\hbar\omega_{\perp}}}{\left(e^{\beta\hbar\omega_{\perp}} - 1\right)^2} d\omega_{\perp} \quad (1b)$$

where ω_D is the Debye Frequency, $\beta = (k_B T)^{-1}$ and in order to get rid of the inadequacies involved due to Matthiessen's rule the relaxation times $\tau_{k\parallel}^{-1}(\omega)$ and $\tau_{k\perp}^{-1}(\omega)$ are along in-plane and cross-plane directions which can be replaced by phonon line widths $\Gamma_{k_{\parallel}}(\omega)$ and $\Gamma_{k_{\perp}}(\omega)$ [18,20,21]. The evolution of $\Gamma_{k_{\parallel}}(\omega)$ and $\Gamma_{k_{\perp}}(\omega)$ can be obtained with the help of quantum dynamics of phonons [20,21,25,26,27,28].

3. The Collision Processes

In order to investigate the many body quantum dynamics to explore the various scattering mechanism, let us consider the Hamiltonian for a HTS in the form

$$H = H_p + H_A + H_e + H_{ep} + H_D \tag{2}$$

where,

$$H_p = \sum_k \frac{\hbar\omega_k}{4}[A_k^* A_k + B_k^* B_k] \tag{2a}$$

$$H_A = \sum_{s\geq 3}\sum_{k_1,..,k_s} \hbar V_s(k_1,k_2,...,k_s) A_{k_1} A_{k_2} .... A_{k_s} \tag{2b}$$

$$H_e = \sum_q \begin{pmatrix} \hbar\omega_{q\uparrow} b_{q\uparrow}^* b_{q\uparrow} + \hbar\omega_{q\downarrow} b_{q\downarrow}^* b_{q\downarrow} \\ +\hbar\omega_{-q\uparrow} b_{-q\uparrow}^* b_{-q\uparrow} + \hbar\omega_{-q\downarrow} b_{-q\downarrow}^* b_{-q\downarrow} \end{pmatrix} \tag{2c}$$

$$H_{ep} = \sum_{k,q} \begin{pmatrix} g_k b_{Q\uparrow}^* b_{q\uparrow} + g_k^* b_{q\uparrow}^* b_{Q\uparrow} \\ +g_k b_{Q\downarrow}^* b_{q\downarrow} + g_k^* b_{q\downarrow}^* b_{Q\downarrow} \end{pmatrix} B_k \tag{2d}$$

$$\begin{aligned} H_D = &-\hbar \sum_{k_1,k_2} \left[C(k_1,k_2) B_{k_1} B_{k_2} \right] \\ &+\hbar \sum_{k_1,k_2} \left[D(k_1,k_2) A_{k_1} A_{k_2} \right]. \end{aligned} \tag{2e}$$

In the above equations the symbols H_p, H_A, H_e, H_{ep} and H_D respectively stand for harmonic phonon- [25], anharmonic phonon- [26,27,28], electron-[29,30], electron-phonon coupling- [29,30,31] and Defect-Hamiltonian [26,28,29,30,31]. This Hamiltonian can be used to evaluate the double time temperature dependent phonon Green's function

$$\begin{aligned} G_{kk'}(t-t') &= \langle\langle A_k(t); A^*_{k'}(t')\rangle\rangle \\ &= -i\theta(t-t')\langle A_k(t), A^*_{k'}(t')\rangle. \end{aligned} \tag{3}$$

in the form

$$G_{kk'}(\omega) = \frac{\omega_k \eta_{kk'}}{\pi[\omega^2 - \tilde{\omega}_k^{\,2} - 2\omega_k \tilde{P}(k,k',\omega)]} \tag{4}$$

here $\tilde{\omega}_k$ is the renormalized phonon frequency and $\tilde{P}(k,k',\omega)$ is the self-energy operator or response function

$$\tilde{P}(k,k',\omega) = Lim_{\varepsilon\to 0^+} \Delta_k(\omega) - i\Gamma_k(\omega) \tag{5}$$

Where $\Delta_k(\omega)$ (real part of $\tilde{P}(k,k',\omega)$) is shift in the phonon frequency and the imaginary part is the phonon frequency line width at the half maximum of the phonon frequency peak and can be written in the form

$$\Gamma_k(\omega) = \Gamma_k^A(\omega) + \Gamma_k^{ep}(\omega) + \Gamma_k^D(\omega) + \Gamma_k^{AD}(\omega) \tag{6}$$

Here $\Gamma_k^D(\omega)$, $\Gamma_k^A(\omega)$, $\Gamma_k^{AD}(\omega)$ and $\Gamma_k^{ep}(\omega)$ are the individual contributions of line widths (life times) due to point defect scattering, phonon-phonon scattering, interference scattering and electron-phonon scattering, respectively, more details of every term are available in the references elsewhere [26,27,28,31] and will be discussed in the rest of the paper.

The relaxation time as per Callaway formalism is given by $\tau^{-1} = \sum_i \tau_i^{-1}$ for i type of scattering processes not interacting with each other which in general is never found in a real system and addresses the wrong application of Matthiessen's rule. The i type of collision events may be described in terms of boundary scattering τ_{CB}^{-1}, impurity scattering $\tau_D^{-1}(\omega)$, phonon-phonon collision $\tau_{ph}^{-1}(\omega)$, interference scattering $\tau_{AD}^{-1}(\omega)$, electron-phonon $\tau_{e-p}^{-1}(\omega)$, resonance scattering $\tau_R^{-1}(\omega)$ events, etc. The problem of use of adequate dispersion relations and the inverse additivity of relaxation times can be resolved by taking the concept of renormalized and perturbed mode frequencies [18,31] and $\tau^{-1} = \Gamma_k(\omega)$ [18,20,21,31] which in accordance with Eq. (1) can be resolved in the form

$$\tau^{-1} = \tau_{k_{\parallel}}^{-1} + \tau_{k_{\perp}}^{-1} = \Gamma_{k_{\parallel}}(\omega) + \Gamma_{k_{\perp}}(\omega) = \Gamma_k(\omega) \tag{7}$$

where

$$\tau_{k_{\|}}(\omega)=\tau_{\|CB}{}^{-1}+\Gamma_{k_{\|}}^{A}(\omega)+\Gamma_{k_{\|}}^{AD}(\omega)+\Gamma_{k_{\|}}^{ep}(\omega)+\Gamma_{k_{\|}}^{D}(\omega)+\tau_{\|R}{}^{-1} \quad (8a)$$

$$\tau_{k_{\perp}}(\omega)=\tau_{\perp CB}{}^{-1}+\Gamma_{k_{\perp}}^{A}(\omega)+\Gamma_{k_{\perp}}^{AD}(\omega)+\Gamma_{k_{\perp}}^{ep}(\omega)+\Gamma_{k_{\perp}}^{D}(\omega)+\tau_{\perp R}{}^{-1}. \quad (8b)$$

Despite of several serious objections in the numerically amenable Callaway model established wide acceptability to successfully analyze thermal conductivity by the use of the concept of the relaxation times which has convoluted dependence on frequency, temperature and various distribution functions in a large number of scattering processes involved and resorts it as a very sensitive quantity. However, this model was greatly modified by a large number of authors to shape it up in a physically justifiable format [1,4,19,20,21,22,23,35]. A brief account of these events for the layered systems is described as follows:

3.1. Combined Boundary Scattering

The concept of boundary scattering phenomenon [15,16,17,18,20,21,31,32] is based on the assumption that at low temperatures the long wavelength phonons of low frequency get excited and scatters from the crystal boundaries at the relaxation rate of $\tau_B{}^{-1}=v/L$ where $L=1.22(l_1l_2)^{1/2}$ is the Casimir length [15] and l_1, l_2 are cross sectional area of the specimen. Some limitations of Casimir theory which enforced to use L as a parameter in most of the work on thermal conductivity and this was modified by considering the involvement of crystal micro boundaries due to micro scale fluctuations in the internal boundaries of the crystal [32] in the form of $\tau_{CB}^{-1}=v_p/L_B$, L_B being the modified Casimir length. Here the term τ_{CB}^{-1} can be modified for the layered systems as $\tau_{CB}^{-1}=\tau_{\|CB}^{-1}+\tau_{\perp CB}^{-1}$, where $\tau_{\|CB}^{-1}=v_{p\|}/L_{\|}(B)$ and $\tau_{\perp CB}^{-1}=v_{p\perp}/L_{\perp}(B)$. These microscale fluctuations incorporated in L_B offer significant resistance for longer wavelengths and strong phonon-boundary scattering is indeed the reason for increased thermoelectric performance of nanostructures and silicon nanowires in particular [33].

3.2. Impurity Scattering

The contribution of scattering from defect events starts as the temperature starts rising and higher frequency phonons begin to excite with shorter wavelengths. Phonons get localized around the impurity sites and interact with impurities offering much thermal resistance. However, the point impurity scattering was described by Klemens [4] for mass change parameter but when one develops the same problem with the help of many body quantum dynamical theory the lifetime can be obtained in the following forms [16-21]

$$\Gamma_k^D(\omega)=8\pi\varepsilon(\omega)\sum_{k1}R(-k,k_1)R^*(-k,k_1)\omega_{k_1}\delta\left(\omega^2-\tilde{\omega}_k{}^2\right) \quad (9)$$
$$\approx A\omega^4+A_1\omega^2$$

It is noteworthy here that apart from the Klemens expression there arises force constant change term depending on square of frequency which of course is highly sensitive in the description of heat capacity. This result can further be obtained for a layered crystal in the form

$$\Gamma_k^D(\omega)=\Gamma_{k_{\|}}^D(\omega)+\Gamma_{k_{\perp}}^D(\omega) \approx A_{m_{\|}}\omega_{\|}{}^4+A_{m_{\perp}}\omega_{\perp}{}^4+A_{1\|}\omega_{\|}{}^2+A_{1\perp}\omega_{\perp}{}^2 \quad (10)$$

$A_j(j=\|,\ \perp)$ being layered system constants. The variation of defect scattering rates with temperature and reduced frequency for in plane and cross plane cases is shown in Figure 1 dissimilar trend for both the cases, i.e., for cross plane defects contribute dominatingly as compared to in plane scenario heralding that the cross plane heat conduction can be limited significantly.

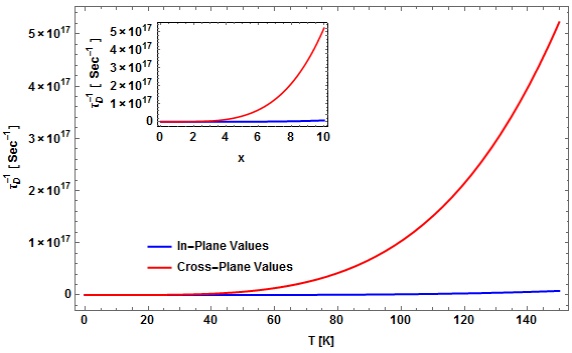

Figure 1. Behavior of τ_D^{-1} vs T [inset τ_D^{-1} vs x] for in-plane and cross-plane references.

3.3. Phonon-Phonon Processes

With further rise in temperature more and more phonons with higher frequencies get excited and start interacting with the cubic and quartic phonon fields of each other giving rise to phonon-phonon scattering. In HTS the quartic phonon scattering does not take place as it is a phenomenon generally operative at high temperatures and one can restrict to $\Gamma_k^A(\omega)=\Gamma_k^{3A}(\omega)$. In the earlier work the phonon-phonon scattering relaxation time was mostly taken to vary arbitrarily with the powers of frequency and temperature and their multiplier coefficients which couldn't justify the physics of the problem. This problem was systematically undertaken to study quantum dynamically [18,20,21,31] and revealed the following exact frequency and temperature dependence:

$$\Gamma_k^{3A}(\omega)=18\pi\varepsilon(\omega)\sum_{k_1,k_2}|V_3(k_1,k_2,-k)|^2\,\eta_1[S_{+\alpha}\omega_{+\alpha}\times\delta(\omega^2-\omega_{+\alpha}{}^2)-S_{-\alpha}\omega_{-\alpha}\delta(\omega^2-\omega_{-\alpha}{}^2)] \quad (11)$$
$$\approx B\omega^2T$$
$$\approx\Gamma_{\|k}^{3A}(\omega)+\Gamma_{\perp k}^{3A}(\omega)\approx B_{\|}\omega_{\|}{}^2T+B_{\perp}\omega_{\perp}{}^2T.$$

Where $B_j\,(j=\|,\ \perp)$ are constants for a layered system.

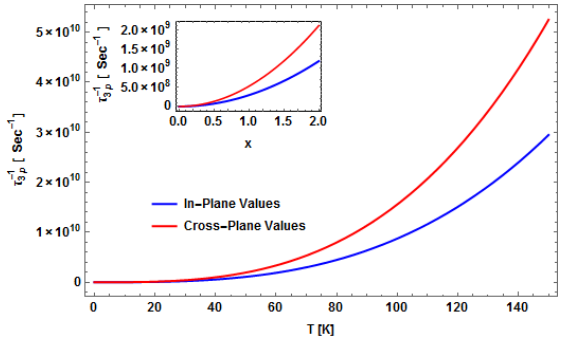

Figure 2. Behavior of τ_{3p}^{-1} vs T [inset τ_{3p}^{-1} vs x] for in-plane and cross-plane references

Figure 2 depicts the variation of phonon-phonon life times in plane and cross plane references with T and x. Apart from defects this scattering infers that the trend for in plane and cross plane cases is similar but the thermal resistance offered by cross planes is certainly higher and may enable one to technological exploitation of the idea that in cross plane direction the system is cold and in the in plane scene it is hot giving way for heat transport.

3.4. Interference Scattering

At elevated temperatures the phonons of localized fields start interacting with those of anharmonic fields giving rise to impurity-anharmonicity interaction modes and interference scattering [18,20,21,31]. Taking these interactions with cubic anharmonicity only the related line width takes the form

$$\begin{aligned}&\Gamma_k^{AD}(\omega)=\Gamma_k^{3D}(\omega)\\&=144\pi\varepsilon(\omega)\sum_{k_1,k_2,k_3}|V_3(k_1,k_2,-k)|^2\ R(k_1,k_2)\omega_k{}^{-1}\eta_1\\&\times[S_{+\alpha}\omega_{+\alpha}\delta(\omega^2-\omega_{+\alpha}{}^2)-S_{-\alpha}\omega_{-\alpha}\delta(\omega^2-\omega_{-\alpha}{}^2)]\\&\approx D\omega^4\approx D_{\|}\omega_{\|}{}^4T+D_{\perp}\omega_{\perp}{}^4T.\end{aligned}\tag{12}$$

This interaction is portrayed in Figure 3 and well prophesied that the cross plane behavior of thermal resistance is much more dominant above the transition temperature as compared to the in-plane heat transport.

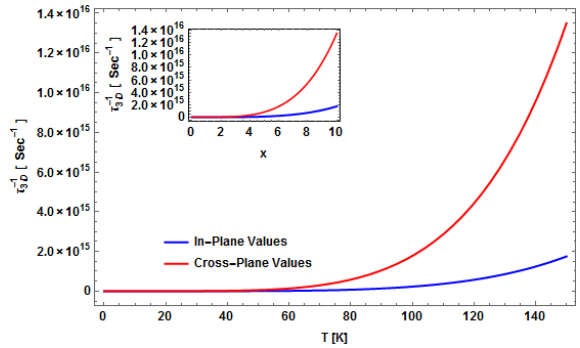

Figure 3. Behavior of τ_{3D}^{-1} vs T [inset τ_{3D}^{-1} vs x] for in-plane and cross-plane references

3.5. Electron-phonon Scattering

Ziman [13] successfully explored the problem of heat transport by electrons which was developed later quantum mechanically [31] and found it a highly sensitive quantity by describing the electron energy line width in the form

$$\begin{aligned}&\Gamma_k^{ep}(\omega)=g^2\omega^2\left[-A_{1e}\left(e^{x/2}+1\right)^{-1}+A_{2e}\coth\left(3x/2\right)\right]\\&\approx g^2\omega_{\|}{}^2\left[-A_{\|1e}\left(e^{x_{\|}/2}+1\right)^{-1}+A_{\|2e}\coth\left(3x_{\|}/2\right)\right]\\&+g^2\omega_{\perp}{}^2\left[-A_{\perp1e}\left(e^{x_{\perp}/2}+1\right)^{-1}+A_{\perp2e}\coth\left(3x_{\perp}/2\right)\right]\end{aligned}\tag{13}$$

with $x=\hbar\omega/k_BT,\ x_j=\hbar\omega_j/k_BT;\ (j=\|,\perp)$. The details of various symbols appearing in the above equations are well described in the references elsewhere [16,17,18,19,20,28,30,32] and needs no reproduction. Electron-phonon interaction events are highly sensitive to the frequency variations and helps in understanding the fact that the pairons or cooper pairs do not contribute to the thermal transport and this typical behavior of electron-phonon events is shown in Figure 3.

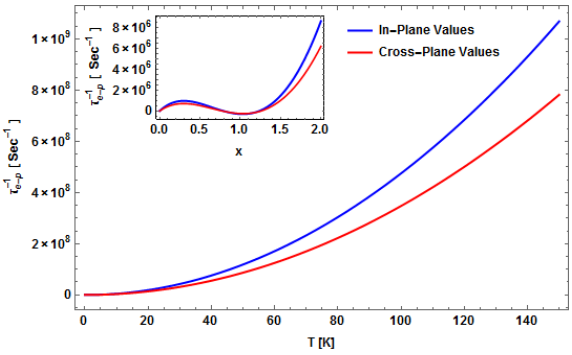

Figure 4. Behavior of τ_{e-p}^{-1} vs T [inset τ_{e-p}^{-1} vs x] for in-plane and cross-plane references

3.6. Resonance Scattering

Pohl [33] associated the dip just above the maximum peak of thermal conductivity with impurity and resonance scattering and the related relaxation rate was described by him is given by

$$\tau_R^{-1}=R\omega^2T^n\left[\left(\omega_0{}^2-\omega^2\right)+\left(\Omega/\pi\right)^2\omega_0{}^2\omega^2\right]^{-1}\tag{14}$$

which gives its form for layered systems as follows:

$$\begin{aligned}&\tau_R^{-1}=R_{\|}\omega_{\|}{}^2T^n\left[\left(\omega_{\|0}{}^2-\omega_{\|}{}^2\right)+\left(\Omega/\pi\right)^2\omega_{\|0}{}^2\omega_{\|}{}^2\right]^{-1}\\&+R_{\perp}\omega_{\perp}{}^2T^n\times\left[\left(\omega_{\perp0}{}^2-\omega_{\perp}{}^2\right)+\left(\Omega/\pi\right)^2\omega_{\perp0}{}^2\omega_{\perp}{}^2\right]^{-1}\end{aligned}\tag{15}$$

where $R_{\|}$, $R_{\perp}$ are the in-plane and cross-plane proportionality constants related to the impurity concentration. $\omega_{0\|}$ and $\omega_{0\perp}$ are respective resonance frequencies and Ω is the damping constant.

4. Analysis of Thermal Conductivity

In order to justify the outcome of the above findings we have taken up the numerical analysis of thermal conductivity of high temperature oxide superconductor La-Sr-Cu-O samples. The experimental results of Uher [5]

for the samples La_2SrCuO_4, $La_{1.8}Sr_{0.2}CuO_4$, and $La_{1.85}Sr_{0.15}CuO_4$ have been taken for the purpose of analysis for different temperature ranges $0-70K$, $0-100K$ and $0-140K$, respectively. The values of various constants and parameters used in the analysis of in-plane and cross-plane thermal conductivity are furnished in Table 1, separately for each sample. The numerical estimation has been carried out in the light of Eqs. (1), (1a) and (1b) have been portrayed in Figure 5 through 7, which reveal excellent agreements between theory and experimental observations throughout all the temperature ranges. The phonon velocity can be replaced by the group velocity $v_p \approx v_g$ which can be further resolved via simplest dispersion relation of the form $\omega^2 = \omega_{\|}^2 + \omega_{\perp}^2 = v_{g_{\|}}^2 k_{\|}^2 + v_{g_{\perp}}^2 k_{\perp}^2$ with $k^2 = k_{\|}^2 + k_{\|}^2$, $k_{\|}^2 = k_x^2 + k_y^2$ and $k_{\perp} = k_z$ in the Debye approximation [18]. This concept is well supported by Holland's two mode analysis [35]. During the numerical computation it is observed that the contribution of combined boundary and impurity scattering events is highly effective at low temperatures but their significance gradually diminishes with the rise of temperature and these processes are eventually replaced by the phonon-phonon scattering and interference processes. The findings of Kristoffel *et al* that the impurities play a very essential role in the cuprate superconductors [36] is well supported in the present work.

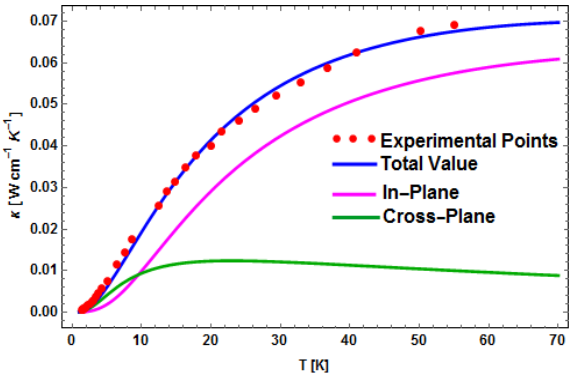

Figure 5. Analysis of thermal conductivity of La_2SrCuO_4 sample

The phonon-phonon interactions and higher order collision events certainly take place in the system when the temperature is continuously elevated resulting in the excitation of higher and higher frequency phonons with considerably smaller wavelength enabling the collisions at smaller distances and the thermal resistance continuously becomes more and more severe. Obviously,

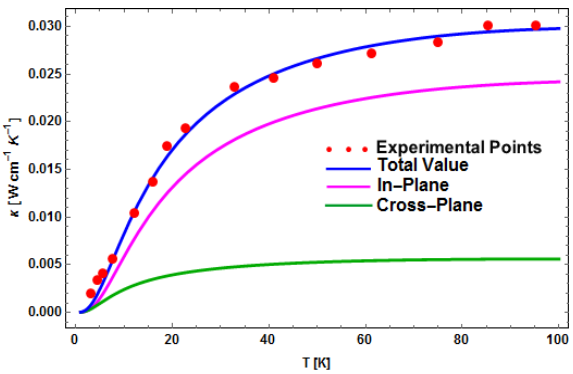

Figure 6. Analysis of thermal conductivity of $La_{1.8}Sr_{0.2}$ CuO_4 sample

The situation becomes so intense that the phonons of anharmonic phonon fields start interacting with the phonons of localized fields giving rise to the interference interactions with higher magnitude of thermal resistance. The varied frequency and temperature dependence for phonon processes by earlier worker at their choice thus gets proper justification through phonon-phonon and interference processes and work at and above the thermal conductivity maxima.

Table 1. Constants and parameters used in the analysis of thermal conductivity of high temperature superconductor $La_{2x}S_xCuO_4$ samples

Sample	La_2SrCuO_4	$La_{1.8}Sr_{0.2}CuO_4$	$La_{1.85}Sr_{0.15}CuO_4$
Tc (K)	37	37	37
θ (K)	410	400	410
$g_{\|}$	0.7	0.7	0.7
$g_{\perp}$	1.6	0.6	0.6
$L_{\|}$(B)$(\times10^{-3}\ cm)$	0.155	0.153	0.155
$L_{\perp}$ (B)$(\times10^{-3}\ cm)$	0.275	0.145	0.145
$A_{m\|}$ $(\times10^{-43}\ s^3)$	17.9197	83.6587	53.6597
$A_{m\perp}(\times10^{-43}\ s^3)$	20.0659	70.6197	350.6197
$B_{\|}$ $(\times10^{-22}\ sK^{-1})$	20.8982	20.8972	50.8982
$B_{\perp}$ $(\times10^{-22}\ sK^{-1})$	218.6982	20.6972	90.6982
$D_{\|}$ $(\times10^{-45}\ s^3K^{-1})$	7.14134	7.14134	7.84134
$D_{\perp}(\times10^{-45}\ s^3K^{-1})$	110.4134	7.41344	60.4134
$v_{\|}$ $(\times10^{5}\ cms^{-1})$	6.2	6.4	7.5
$v_{\perp}$ $(\times10^{5}\ cms^{-1})$	4.0	6.1	7.5
$A_{\|1e}(\times10^{2}erg^{-2}K^{-2})$	9.89	9.89	9.89
$A_{\perp1e}(\times10^{2}erg^{-2}K^{-2})$	19.89	2.091	9.89
$A_{\|2e}(\times10^{2}erg^{-2}K^{-2})$	9.8909	9.89	9.89
$A_{\perp2e}(\times10^{2}erg^{-2}K^{-2})$	19.85	2.07	9.85
$R_{\|}$ $(\times10^{32}s^3)$	-	-	0.80
$R_{\perp}$ $(\times10^{32}s^3)$	-	-	1.41
$\omega_{\|0}$ $(\times10^{12}s^{-1})$	-	-	3.11
$\omega_{\perp0}$ $(\times10^{12}s^{-1})$	-	-	3.05

The electron-phonon interactions primarily participate in the thermal transport above the conductivity maximum in the case of high temperature superconductors where conductivity curve shows a cusp like trend near the transition temperature. This cusp is more and more pronounced in case of YBaCuO superconductors [5,31,37].

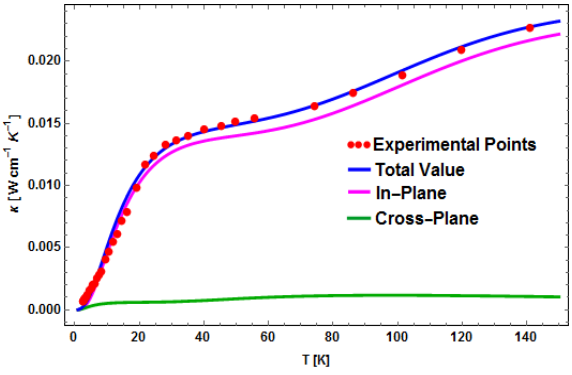

Figure 7. Analysis of thermal conductivity of $La_{1.85}Sr_{0.15}CuO_4$ sample

Since the pairons are generated as a result of phonon mediated effects of electrons and never contribute in the

thermal transport and may be attributed to negative thermal resistance (Figure 4 inset) in this region giving cusp like behavior.

Coming to the case of in plane and cross plane thermal transport the various parameters used in computation show that in plane values are always smaller than those of cross plane values. Before going into further details let us define the thermal conductivity functions for in-plane $\zeta_{\|}$ and cross-plane $\zeta_{\perp}$ contributions as

$$\zeta_{\|} = \frac{k_B \beta^2 \hbar^2 \omega_{\|}{}^4 e^{\beta\hbar\omega_{\|}}}{2\pi^2 v_{\|}\, \Gamma_k(\omega_{\|}, T)\left(e^{\beta\hbar\omega_{\|}} - 1\right)^2} \tag{16a}$$

$$\zeta_{\perp} = \frac{k_B \beta^2 \hbar^2 \omega_{\perp}{}^4 e^{\beta\hbar\omega_{\perp}}}{2\pi^2 v_{\perp}\, \Gamma_k(\omega_{\perp}, T)\left(e^{\beta\hbar\omega_{\perp}} - 1\right)^2}. \tag{16b}$$

The variation of conductivity function for in-plane and cross plane have been portrayed with $x_{\|}$, T is depicted in Figure 8 and Figure 9.

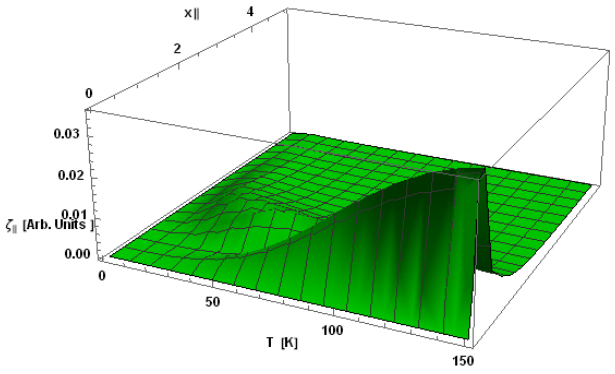

Figure 8. Variation of in-plane thermal conductivity function $\zeta_{\|}(x_{\|}, T)$ versus $x_{\|}$ and T for all collision process

For reduced frequencies between $x_j < 1$ the thermal conductivity function shows sharp peak and the behavior becomes more pronounced at higher temperatures and as is clear from contour lines at the frequencies $x_j > 1$ the contribution remains almost constant, notably the curve flattens very rapidly in case of cross plane reference.

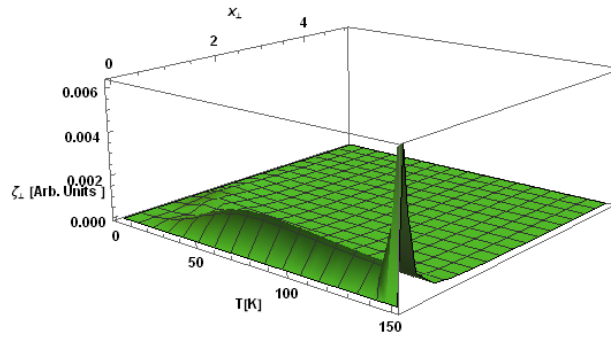

Figure 9. Variation of cross-plane thermal conductivity function $\zeta_{\perp}(x_{\perp}, T)$ versus $x_{\perp}$ and T for all collision process

The curves in Figure 5 – Figure 7 show that the nature of $\kappa_{\|}$ almost follows the nature of experimental curves but the behavior of $\kappa_{\perp}$ is completely different and slightly rising trend at initial low temperatures but immediately becomes constant for elevated temperatures inferring that it becomes least temperature sensitive.

5. Conclusions

Present investigations successfully describe the behavior of thermal conductivity of cuprate superconductors and is applicable to the all types of high temperatures superconductors. Further, the present study supports that the thermal conductivity in both directions i.e. parallel to the layers and perpendicular to the layers is always smaller than that of bulk materials. It is also inferred that the thermal transport is quite efficient parallel to the layers and along the growth axis or in the cross-plane direction is found quite small compared to the in-plane direction of $La_{2-x}Sr_xCuO_4$ superconductors. This idea can be technologically exploited in fabrication/design of the devices in which the system should not respond to temperature in a particular direction whereas shows maximum response to temperature in the rest of the directions. In other words, the theory concludes that it is possible to develop the devices which is hot in the in plane direction but cold in the cross plane direction.

References

[1] Bardeen, J., Rickayazen G. and Tewordt L., Theory of the thermal conductivity of superconductors, *Phys. Rev. B*, 113, 982-994, 1959.

[2] Callaway, J., Model for lattice thermal conductivity at low temperatures, *Phys. Rev*., 113, 1046-1051, 1959.

[3] Parrott, J. E. and Stukes, A. D., *Thermal conductivity of solids*, Pion Limited, London, 1975.

[4] Klemens, P. G., Thermal conductivity and lattice vibrational modes, *Sol. Stat. Phys*., 7, 1-98, 1958.

[5] Uher, C., Thermal conductivity of High T_c Superconductors, *J. Superconductivity*, 3, 337-389, 1990.

[6] Cahill, D. G., Goodson, K., and Majumdar, A., Thermometry and Thermal Transport in Micro/ Nanoscale Solid-State Devices and Structures, *J. Heat Trans.*, 124, 223-241, 2002.

[7] Cahill, D. G., Ford, W. K., Goodson, K.E., Mahan, G. D., Majumdar, A., Maris H. J., Merlin, R., and Phillpot, S. R., Nanoscale Thermal Transport, *J. Appl. Phys.*, 93, 793-818, 2003.

[8] Mahan, G.D., *Thermal Conductivity*, edited by Terry M. Trit, Kluwer Academic/Plenum Publishers, New York, 1-285, 2004.

[9] Narayanamurti, V., Stormer, H. L., Chin, M. A., Gossard, A.C., and Wiegmann, W., Selective Transmission of High-Frequency Phonons by a Superlattice: The dielectric Phonon Filter, *Phys. Rev. Lett.*, 43, 2012-2016, 1979.

[10] Varshney, D., Chaudhry, K. K. and Singh, R. K., Analysis of in-plane thermal conductivity anomalies in $YBa_2Cu_3O_{7-\delta}$ cuprate Superconductors, *New J. Phys.*, 5, 72.1-72.17, 2003.

[11] Klemens, P. G., The scattering of low-frequency lattice waves by static imperfections, *Proc. Phys. Soc. A*, 68, 1113-1128, 1955.

[12] Carruthers, P., Theory of thermal conductivity of solids at low temperatures, *Rev. Mod. Phys*., 33, 92-138, 1961.

[13] Ziman, J. M., *Electrons and Phonons*, Clarendon Press, Oxford, U. K., 1962.

[14] De Hass, W. J., Biermasz, T., Thermal conductivity in diamond and potassium chloride, *Physica* 5 , 47-53, 1938.

[15] Casimir, H. B. G., Note on the Conduction of Heat in Crystals, *Physica*, 5, 495-500, 1938.

[16] Hyldgaard, P., and Mahan, G. D., Phonon Superlattice Transport, *Phys. Rev. B*, 56, 10754-10757, 1997.

[17] Chen, G., Size and Interface Effects on Thermal Conductivity of Superlattices and Periodic Thin-Film Structures, *J. Heat Trans*., 119, 220-229 1997.

[18] Saini Richa, Ashokan Vinod, Indu, B.D., Phonon conduction in superlattices, *Superlattices and Microstructures*, 82, 574-583, 2015.

[19] Erdos, P., and Halley, S. B., Low-Temperature Thermal Cond--uctivity of Impure Insulators, *Phys. Rev.*,184 , 951-967, 1969.

[20] Gairola, R. P., Low-Temperature Lattice Thermal Conductivity of Nonmetallic Solids with Isotopic Impurities, *Phys. State Solidi B*, 125, 65-74, 1984.

[21] Bahuguna, B.P., Painuli, C. P. , and Indu, B. D., Phonon Heat Con-ductivity of Garnets Containing Rare Earth Ions, *Acta Phys. Pol. A*, 80, 527-554, 1991.

[22] Ward, A., and Broido, D. A., Intrinsic lattice thermal conductivity of Si/Ge and GaAs/AlAs superlattice, *Phys. Rev.* B, 77, 245328-1-7, 2008.

[23] Broido, D. A., Ward, A. and Mingo, N., Lattice thermal conductivity of silicon from empirical interatomic potentials, *Phys. Rev.* B, 72 , 014308-1-8, 2005.

[24] Ward, A., Ab initio theory of the lattice thermal conductivity in diamond, *Phys. Rev.* B, 80, 125203-1-8, 2009.

[25] Pathak, K. N., Theory of anharmonic crystals., *Phys. Rev.*, 139, A1569-A1580, 1965.

[26] Sharma, P.K., and Bahadur, R., Thermal Conductivity for Phonon Scattering by Substitutional Defects in Crystals, *Phys. Rev. B*, 12, 1522-1530, 1975.

[27] Indu, B. D, Theory of lattice specific heat of an isotopically disordered anharmonic crystal, *Int. J. Mod. Phys. B*, 4, 1379-1393, 1990.

[28] Indu, B. D, Enhanced phonon density of states in impure anharmonic crystals, *Mod. Phys. Lett. B*, 6, 1665-1672, 1992.

[29] Frohlich, H., *New perspective in modern physics*, edited by R. E. Marshak , John Wiley, New York, 1966.

[30] Fan, H. Y., *Elements of solid state physics*, John Wiley, New York, 1987.

[31] Ashokan, V., Indu, B. D. and A. Kr. Dimri, Signature of electron phonon interaction in high temperature superconductors, *AIP Advances*, 1, 032101-1-032101-16, 2011.

[32] Indu, B. D., Low temperature lattice thermal conductivity of Mg_2 Sn, Mg_2Si, and Mg_2Ge, Nuovo *Cimento* B, 58, 345-350, 1980.

[33] Hochbaum, A., Chen, R., Delgado, R., W., Liang, Garnett, E., Najarian, M., Majumdar, A., and Yang, P., "Enhanced Thermoelectric Performance of Rough Silicon Nanowires", *Nature*, 451, 163-167, 2008.

[34] Pohl, R. O., Thermal Conductivity and Phonon Resonance Scattering, *Phys. Rev. Lett*., 8, 481-483, 1962.

[35] Holland, M.G., Analysis of thermal conductivity, *Phys. Rev.*, 132, 2461-2471, 1963.

[36] Kristoffel, N. and Rubin, P., Localized electron levels of cuo2 planes perturbed by detects in high-Tc superconductors, *Rev. Solid State Sci.*, 5, 449-460,1991.

[37] Ashokan, V. and Indu, B.D., Theory of thermal conductivity of high temperature superconductors: a new approach, *Mod. Phys. Letters B*, 25, 663-678, 2011.